Toxicology and Applied Pharmacology 272 (2013) 399–407

Contents lists available at ScienceDirect

Toxicology and Applied Pharmacology

journal homepage: www.elsevier.com/locate/ytaap

Human stem cell osteoblastogenesis mediated by novel glycogen synthase kinase 3 inhibitors induces bone formation and a unique bone turnover biomarker profile in rats ☆☆

Peter S. Gilmour [a,*], Patrick J. O'Shea [a], Malbinder Fagura [a], James E. Pilling [b], Hitesh Sanganee [a], Hiroki Wada [c], Paul F. Courtney [d], Stefan Kavanagh [e], Peter A. Hall [e], K. Jane Escott [a]

[a] New Opportunities Innovative Medicines group, AstraZeneca R&D, Alderley Park, Cheshire SK10 4TF, UK
[b] Discovery Sciences, AstraZeneca R&D, Alderley Park, Cheshire SK10 4TF, UK
[c] R&I IMed, AstraZeneca R&D, Molndal, Sweden
[d] DMPK, AstraZeneca R&D, Alderley Park, Cheshire SK10 4TF, UK
[e] Safety Assessment, AstraZeneca R&D, Alderley Park, Cheshire SK10 4TF, UK

ARTICLE INFO

Article history:
Received 24 April 2013
Revised 25 June 2013
Accepted 4 July 2013
Available online 18 July 2013

Keywords:
Wnt
β-catenin
Stromal/stem cells
In vivo
Biomarkers
Bone turnover

ABSTRACT

Wnt activation by inhibiting glycogen synthase kinase 3 (GSK-3) causes bone anabolism in rodents making GSK-3 a potential therapeutic target for osteoporotic and osteolytic metastatic bone disease. To understand the wnt pathway related to human disease translation, the ability of 3 potent inhibitors of GSK-3 (AZD2858, AR79, AZ13282107) to 1) drive osteoblast differentiation and mineralisation using human adipose-derived stem cells (hADSC) *in vitro*; and 2) stimulate rat bone formation *in vivo* was investigated. Bone anabolism/resorption was determined using clinically relevant serum biomarkers as indicators of bone turnover and bone formation assessed in femurs by histopathology and pQCT/μCT imaging.

GSK-3 inhibitors caused β-catenin stabilisation in human and rat mesenchymal stem cells, stimulated hADSC commitment towards osteoblasts and osteogenic mineralisation *in vitro*. AZD2858 produced time-dependent changes in serum bone turnover biomarkers and increased bone mass over 28 days exposure in rats. After 7 days, AZD2858, AR79 or AZ13282107 exposure increased the bone formation biomarker P1NP, and reduced the resorption biomarker TRAcP-5b, indicating increased bone anabolism and reduced resorption in rats. This biomarker profile was differentiated from anabolic agent PTH_{1-34} or the anti-resorptive Alendronate-induced changes. Increased bone formation in cortical and cancellous bone as assessed by femur histopathology supported biomarker changes. 14 day AR79 treatment increased bone mineral density and trabecular thickness, and decreased trabecular number and connectivity assessed by pQCT/μCT.

GSK-3 inhibition caused hADSC osteoblastogenesis and mineralisation *in vitro*. Increased femur bone mass associated with changes in bone turnover biomarkers confirmed *in vivo* bone formation and indicated uncoupling of bone formation and resorption.

Introduction

The process of bone remodelling involves tightly coupled bone resorption and formation activities and dysregulation of bone turnover can lead to a number of bone disorders such as osteopetrosis and osteoporosis. In malignant diseases, bone destruction through increased bone resorption produces osteolytic lesions and is a characteristic feature of multiple myeloma and breast cancer metastatic disease (Theriault, 2012). Current therapies aimed for osteoporotic and osteolytic bone diseases are primarily aimed at reducing bone resorption. However, stimulating anabolic activity is an alternative and complementary therapeutic strategy. Therefore, understanding of the biochemical pathways governing osteoblast differentiation and function has aided the search for anabolic therapies and recent research has highlighted the importance of Wnt signalling in bone formation. Canonical Wnt signalling is critical for osteoblast maturation and function and activation of Wnt signalling through inhibition of constitutively active GSK-3 results in induction of β-catenin and Runx2 transcriptional activities (Hartmann, 2006; Kugimiya et al., 2007; Monroe et al., 2012; Reinhold and Naski, 2007). *In vitro*, GSK-3 inhibition leads to osteoblast differentiation in a C3H10T1/2 murine mesenchymal stem cell (MSC)

☆☆ Disclosures: All authors are employees of AstraZeneca at the time of submission of this manuscript.

* Corresponding author at: New Opportunities iMed, AstraZeneca R&D, Alderley Park (11F, 124-3), Cheshire SK10 4TF, UK.
E-mail address: Peter.Gilmour@astrazeneca.com (P.S. Gilmour).

0041-008X
http://dx.doi.org/10.1016/j.taap.2013.07.001

population (Kulkarni et al., 2006). Accordingly *in vivo*, haploinsufficient GSK-3β mice display increased bone density in comparison to wildtype mice (Kugimiya et al., 2007) and small molecule inhibitors of GSK-3α/β have demonstrated increased bone mass in normal and ovariectomized rodent models (Clement-Lacroix et al., 2005; Gambardella et al., 2011; Kulkarni et al., 2006; Marsell et al., 2012).

In order to determine the role of GSK-3 in human osteoblastogenesis, three structurally diverse, potent GSK-3 inhibitors were tested in hADSC assays *in vitro*. We have assessed the ability of these GSK-3 inhibitors to stimulate canonical Wnt/β-catenin signalling through β-catenin stabilisation and osteogenic mineralisation. In addition, we have studied the commitment of hADSC towards osteoblastogenesis through the assessment of protein transcriptional co-activator with PDZ-binding motif (TAZ), and the osteoblast-specific marker Osterix. TAZ modulates the activity of the critical osteoblast transcription factor runt-related transcription factor 2 (RUNX2) and PPARγ during MSC lineage commitment (Hong et al., 2005) and has recently been reported as a downstream component of the Wnt/β-catenin signalling cascade (Azzolin et al., 2012). Osterix has been reported to be essential for osteoblast differentiation and bone formation as exemplified by the complete lack of osteoblast differentiation and maturation in osterix-null mice (Nakashima et al., 2002). In order to demonstate translation of these *in vitro* findings to bone anabolism in an intact system, each GSK-3 inhibitor was dosed daily to rats, and bone formation *in vivo* was investigated by quantifying changes in serum biomarkers of bone turnover and femur bone changes. One challenge for pre-clinical assessment of potential bone anabolic agents is the ability to measure changes over a short period of time in *in vivo* models as many agents that modulate bone turnover have been tested in lengthy disease models such as the ovariectomized rat model. Therefore, serum bone turnover markers, which are used in the clinical setting, were used in these studies to evaluate treatment effectiveness before mature bone formation could be observed in healthy rats. Initially, a time course of changes in serum bone turnover biomarkers was established following daily dosing of AZD2858 which has known anabolic activity in rats (Marsell et al., 2012). Then, the effect of three different GSK-3 inhibitors (AZD2858, AR79 and AZ13282107), PTH_{1-34} and Alendronate on serum biomarkers in short term rat studies (7 days) were assessed by quantifying N-terminal propeptide of type I procollagen (P1NP), a marker of bone anabolism (Hale et al., 2007) and osteoblast activity and Tartrate-resistant acid phosphatase (TRAcP-5b) a marker of bone metabolism (Halleen et al., 2006). In addition, confirmation of bone formation was assessed using histology and imaging (pQCT, μCT) of femurs.

Materials and methods

Small molecule compounds AR79, AZD2858 and AZ13282107 were synthesised at AstraZeneca R&D, Loughborough UK (structures in Fig. 1).

GSK-3 and kinase selectivity assays. The potency of compounds at GSK-3β and cyclin-dependent protein kinase 2 (CDK2, kinase with closest homology to GSK-3β) was assessed using Z-LYTE™ Kinase assay kit (Invitrogen, UK) in the presence of 7 and 80 μM ATP respectively. A ratiometric method was used to calculate the ratio of donor emission (445 nm) to acceptor emission (520 nm) after excitation of the donor fluorophore at 400 nm to quantitate the reaction progress. Kinase selectivity with AR79, AZD2858 and AZ13282107 were determined using the KinaseProfiler Service (Millipore, Watford, UK) or University of Dundee Kinase (MRC Protein Phosphorylation Unit, UK). Over 80 different kinases were assessed at a single concentration of 1 or 10 μM of AR79, AZD2858 and AZ13282107. Concentration-inhibition 10-point curves to compounds that showed activity were constructed to determine pIC_{50} estimations. Also, in some kinase assays these pIC_{50} estimations were converted to binding affinity values (pK_i) using the Cheng–Prussoff equation to correct for the concentration of ATP used.

β-catenin stabilisation in mesenchymal stem cells. Human adipose-derived stem cells (hADSC; Invitrogen, UK) and rat MSCs (isolated from bone marrow of Sprague Dawley rats at ≤8 weeks after gestation; Invitrogen, UK) were cultured in a basal media of Dulbecco's Modified Eagle's Medium (DMEM; Sigma-Aldrich, UK) containing 5% (v/v) foetal bovine serum (FBS, Gibco, UK) and 2 mM GlutaMax (Invitrogen, UK). Cells were seeded in basal media into 96-well plates (3–5000 cells/well) for 18 h before treatment with AZD2858, AR79 or AZ13282107 (0.3 nM to 20 mM). After 24 h, β-catenin stabilisation was measured as previously described (Gambardella et al., 2011).

Osteoblast-specific marker expression. hADSC were seeded at a density of 5000 cells/well into black 96-well Viewplates (Perkin-Elmer Inc., UK) in basal media (as detailed above). All cells were incubated at 37 °C in 5% CO_2/95% air humidified atmosphere. After overnight incubation, basal media was replaced and compounds, at concentrations of 6 nM to 20 μM, or 0.2% DMSO vehicle were added. After 18 h, cells were fixed in 4% paraformaldehyde (PFA) for 20 min followed by washing in PBS. The cells were blocked in PBS supplemented with 1.1% BSA (Sigma-Aldrich) and 0.2% Triton X-100 for 30 min at room temperature. Anti-osterix (1:50 dilution, ab22552, Abcam, UK) and TAZ antibody (1:500 dilution, #2149, Cell Signalling Technology) were added overnight at 4 °C in blocking buffer, followed by addition of Alexa Fluor AF647 donkey anti-rabbit IgG (Invitrogen, UK) and 1 μM Hoechst 33342 in blocking buffer for 1 h at room temperature. Cells were washed and stored in PBS at 4 °C prior to image acquisition and analysis, using an in-built object intensity algorithm, on an IN Cell Analyzer 3000 platform (Amersham Biosciences, UK).

Osteogenic differentiation studies — Alizarin Red staining and automated image analysis. hADSC were seeded at a density of 5000 cells/cm^2 and were cultured in basal media (as above). After overnight incubation, basal media was replaced and compounds were added. In osteogenic positive control wells, basal media was replaced with an osteogenic differentiation media: phenol red-free DMEM supplemented with 5% FBS, 2 mM GlutaMax, 50 μg/ml L-ascorbic acid (Sigma-Aldrich, UK), 5 mM β-glycerophosphate (Calbiochem, UK), and 10 nM dexamethasone (Sigma-Aldrich, UK). Cells were incubated at 37 °C in 5% CO_2 with media and compounds being replaced every 3–4 days over a 25–28 day time-course. Osteogenic mineralisation was visualised using Alizarin Red staining. Cells were washed with PBS followed by

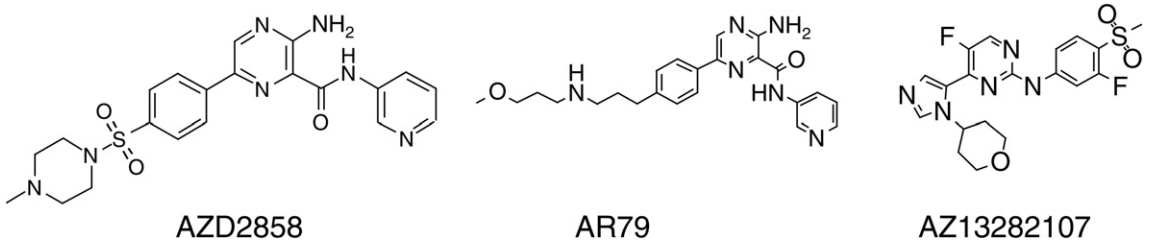

Fig. 1. Small molecule GSK-3 inhibitors from 3 chemical series.

fixation with 4% paraformaldehyde for 20 min at room temperature. The cells were washed three times with PBS before staining with 40 mM Alizarin Red S solution (pH 4.2) for 20 min at room temperature. After staining, cells were washed three times with PBS, followed by washes with water to remove non-specific staining. Plates were allowed to dry and mineralisation was imaged, at 7.3× magnification, using a Leica M165 FC stereomicroscope. Image analysis was performed using custom-designed analysis algorithms created using Definiens Developer XD analysis software (Definiens AG, Germany). Briefly, mineralisation was quantified using a combination of pixel contrast, intensity values, and segmentation in the red channel allowing individual pixels to be classified as either background (white pseudocolour), unstained osteoblast (light blue pseudocolour), or mineralized matrix (medium/dark blue pseudocolour).

Animals and in vivo study protocols. Female Han Wistar (HW) and Sprague–Dawley (SD) rats (240 to 330 g initial weight) were supplied by Harlan, UK and Charles River, UK, group housed and acclimatised for at least 7 days with access to food and water *ad libitum*. Mature animals (>11 weeks) were used in these studies to provide a consistent level of background bone turnover in the absence of rapid adolescent growth and animals in each experiment were matched for size and age. All experimental procedures were performed in accordance with UK Home Office regulations under the Animals (Scientific Procedures) Act 1986. GSK-3 inhibitors were administered by oral gavage, once-a-day (UID) following formulation in either water adjusted to pH 3.5 for AZD2858, or water containing 0.5% HPMC (hydroxypropyl)methyl cellulose, Sigma, Poole, UK) and 0.1% Tween 80 (v/v) (Sigma, Poole, UK) for AR79 and AZ13282107. PTH_{1-34} and alendronate were dissolved in saline and dosed sub-cutaneously (sc). To establish suitable doses, plasma levels of AZD2858, AR79 and AZ13282107 were quantified following a single, oral dose in rats (data not shown). Doses of AR79 and AZ13282107 were calculated based on achieving a similar plasma AUC over 24 h to AZD2858 (30 μmol/kg/day, dose shown to stimulate bone formation in rats Fig. 4). Differences in potency and plasma protein binding between compounds were taken into account when calculating doses. PTH_{1-34} was administered at 30 μg/kg (sc) every second day based on bone anabolism reported previously with intermittent dosing of PTH in this dose range (Fukata et al., 2004). A daily 30 μg/kg (sc) dose of alendronate was used which has been shown to increase bone mineral density in a rat arthritis model (Harada et al., 2004). *In vivo* studies were designed with time-matched, vehicle treated control groups and 8–10 animals per group, randomised by weight. Group sizes were used to give a minimum 80% power to detect 30% change in the biomarker endpoint. Study 1: 28 day time course with AZD2858. Naïve HW rats were dosed by orally, UID for 3, 7, 14, 21 or 28 days with AZD2858 (30 μmol/kg/day) or vehicle (pH3.5 adjusted H_2O). Endpoints were determined 24 h following the final dose. Study 2: 7 day biomarker study with GSK-3 inhibitors AR79, AZ13282107, PTH_{1-34} and Alendronate. Naïve SD rats were dosed with AR79 (11, 32 and 106 μmol/kg/day) or AZ13282107 (7, 23 and 69 μmol/kg/day) orally, UID for 7 days. PTH_{1-34} (once every two days) and alendronate (UID) were dosed (sc) at 30 μg/kg. Study 3: 14 day biomarker and imaging studies with AR79 (32 μmol/kg/day).

Tissue and blood sampling, analysis of compound levels and serum bone biomarkers. All animals were fasted for 16 h prior to termination. Rats were euthanized by intra-peritoneal injection of pentobarbitone sodium (Euthatal). Blood was collected 24 h after final compound dose and serum was prepared for quantification of P1NP and TRAcP-5b by ELISA (IDS Ltd, UK). Terminal pharmacokinetic (PK) blood samples in EDTA were taken from the abdominal vena cava of animals and centrifugation at 12,000 rpm for separation of plasma. Compound levels were determined by preparing ten standard and three quality control (QC) samples covering a range of compound concentrations between 1 and 1000 ng/ml in blank SD rat plasma sample. These plasma samples along with those from dosed animals were prepared by methanolic precipitation of proteins. Following centrifugation, supernatants were analysed by UPLC–MSMS mass spectrometry. Standards and QC's were within ± 20% of nominal concentration, and linear least-squares regression with a 1/× weighting of the peak area ratios (analyte/IS) *versus* the nominal concentration of the calibration standards was used to construct calibration curves. Concentrations of compound in plasma samples taken from dosed rats were calculated using the calibration curves. Left femurs were harvested and fixed in 10% neutral buffered formalin (NBF) prior to histology slide preparation. In some studies, right femurs were harvested, stored in 10% NBF and retained for pQCT (peripheral quantitative computed tomography) and μCT (micro-computed tomography) evaluation.

Slide preparation for histopathology. The left femurs underwent a rapid decalcification process for preparation of haematoxylin and eosin stained sections. The left femurs were fixed in 10% NBF (Pioneer Chemicals, UK) for 10 days followed by a 5 day decalcification in 10% formic acid in water (Fisher Scientific, UK), changing the decalcifying solution daily. Sections 4 μm thick, were cut and stained with haematoxylin and eosin (H&E). An in-house image analysis programme, developed and validated using the Zeiss KS400 system (Carl Zeiss Ltd), was used for the analysis of bone mass within metaphysis regions of haematoxylin and eosin stained sections of rat femur (see Supplementary Fig. S2).

pQCT/μCT femur analysis. Mineral density and cross-sectional dimensions of bone were measured using pQCT (Tuukkanen et al., 2000), namely using Norland Stratec XCT Research SA+ equipment with a Stratec software version 6.0 (Norland Stratec Medizintechnik, Birkenfeld, Germany). The pQCT measurements were performed *ex vivo* from metaphysis (especially trabecular bone) and diaphysis (cortical bone) of each right femur with a voxel size of 0.07 × 0.07 × 0.5 mm^3. See Supplementary Fig. S3 for μCT analysis.

Statistical analysis. For *in vitro* osteogenic mineralisation studies, data were expressed as mean ± SEM. The differences between groups were examined for statistical significance using one-way analysis of variance followed by Tukey's multiple comparison post hoc test, p values <0.05 were considered significant. For *in vivo* studies, each endpoint measured per animal was averaged across each treatment group and the results expressed as mean ± SEM. Results between treatment groups were compared using non-parametric two-tailed Mann–Whitney or Wilcoxon statistical tests as appropriate with a 5% significance level. For histopathology assessment, the pathologist was blinded to the treatment groups.

Results

GSK-3 potency, β-catenin stabilisation and selectivity

AZD2858, AR79 and AZ13282107 are potent GSK-3 inhibitors derived from 3 chemical series (Fig. 1, Table 1). All 3 compounds have similar potency at both GSK-3β and GSK-3α enzymes and cause an increase in β-catenin stabilisation in human and rat MSCs (Table 1, Supplementary Fig. S1). These effects on β-catenin stabilisation are consistent with activation of the canonical wnt signalling pathway since the inhibition of constitutively active GSK-3β prevents β-catenin phosphorylation, ubiquitination and subsequent proteosomal degradation. Each compound was tested for selectivity against >80 different kinases at a single concentration of 1 or 10 μM and off-target hits are summarised in Table 1. AZD2858 is >70 fold selective for other kinases, receptors and enzymes. Less than 100 fold selectivity was observed for AR79 at the following kinases: HIPK2 (no selectivity), PKD1 (8 fold), PIM3 (12 fold) and DYRK1A (24 fold) compared to GSK-3β potency. AZ13282107 was 200 fold selective to CDK2 and did not show activity against other targets tested.

Table 1
Potency and selectivity of AR79, AZD2858 and AZ13282107 (AZ107). Results expressed as mean ± SEM, nM, n = 2–5.

Assay	Parameter	AR79	AZD2858	AZ107
Affinity for target				
Human GSK-3β enzyme	K_i (measured)	3.2 ± 0.8	5[a]	3.2 ± 0.5
Human GSK-3α enzyme	IC_{50}	5.5	0.9[a]	3.5 ± 0.3
Kinase selectivity				
CDK2	K_i	1000 ± 0.97	>800 nM	631 ± 0.93
HIPK2	IC_{50}	11	717[a]	IA @ 1 μM
PKD1 (PKCmu)	IC_{50}	62	85% @ 1 μM	IA @ 1 μM
PIM3	IC_{50}	40	1269[a]	IA @ 1 μM
DYRK1A	IC_{50}	79	64% @ 1 μM	IA @ 1 μM
PRK2	IC_{50}	631	>30000[a]	IA @ 1 μM
FLT1	IC_{50}	3981	94% @ 10 μM	IA @1 μM
Fold selectivity to other kinases vs GSK-3β		1× HIPK2	143× HIPK2	–
		282× CDK2	329× CDK2	200× CDK2
β-catenin stabilisation:		416 ± 97	390 ± 45	482 ± 41
Human adipose stem cell	EC_{50}			
Rat mesenchymal stem cells	EC_{50}	611 ± 81	234 ± 69	265 ± 20
Bone mineralisation:	% increase	417.5 ± 15.3 @ 300 nM	230.9 ± 6.8 @ 200 nM	395.5 ± 30.0 @ 300 nM
Human adipose stem cell				

[a] (Gambardella et al., 2011), inactive (IA) defined as <40% inhibition.

Expression of osteogenic markers

To investigate whether GSK-3 inhibition influenced osteogenic differentiation in hADSC, we used immunofluorescence and automated image analysis to determine the relative protein expression of the osteogenic markers TAZ and osterix following treatment with AZD2858, AR79, and AZ13282107 (Fig. 2). After 18 h treatment, TAZ expression was increased 1.3-, 1.4-, and 1.5-fold by AZD2858 (EC_{50} = 440 nM), AR79 (EC_{50} = 5 nM), and AZ13282107 (EC_{50} = 809 nM), respectively, relative to DMSO vehicle controls. In addition, osterix expression was

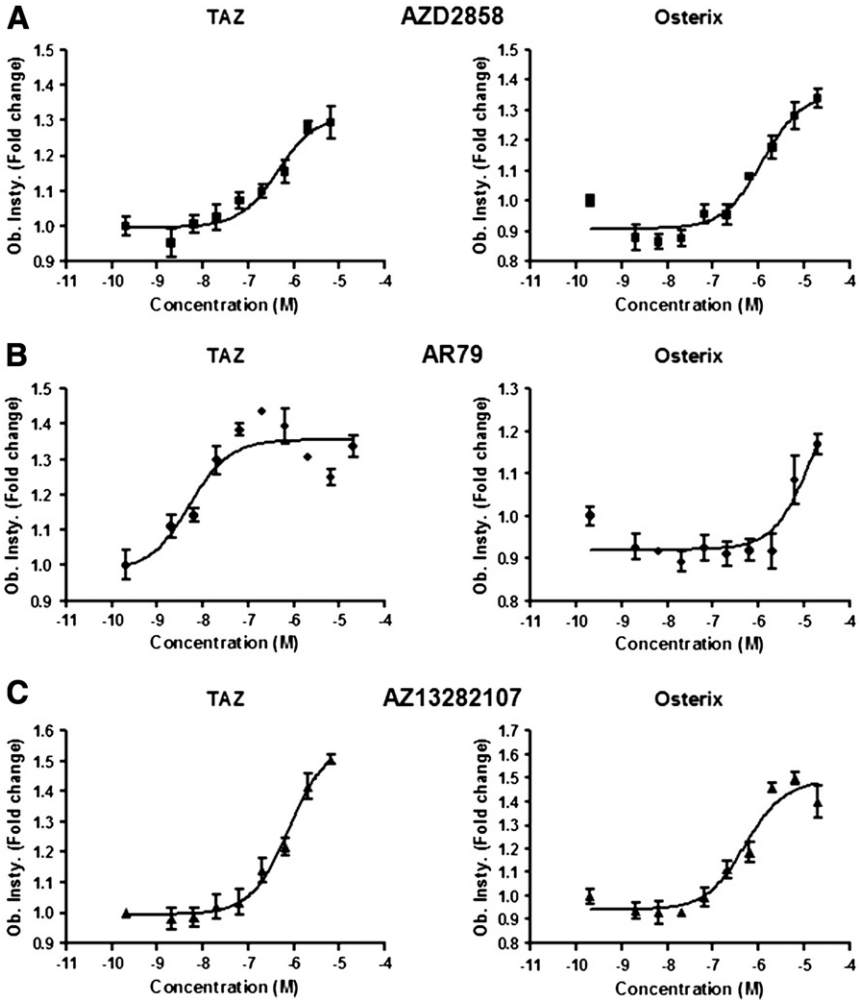

Fig. 2. Expression of TAZ and Osterix, markers of commitment to osteoblastogenesis in human ADSC. Treatment (18 h) with 6 nM to 20 μM of (A) AZD2858, (B) AR79 and (C) AZ13282107, or 0.2% DMSO vehicle. Results expressed as mean ± SEM, n = 3.

increased 1.4-, 1.2-, and 1.5-fold in response to treatment with AZD2858 (EC_{50} = 1.2 μM), AR79, and AZ13282107 (EC_{50} = 501 nM), respectively, relative to DMSO vehicle controls. Taken together, these data demonstrate that inhibition of GSK-3 stimulates osteoblastogenesis in hADSC.

Effect of GSK-3 inhibitors on osteogenic differentiation in hADSC

To investigate the role of Wnt/β-catenin activation in the differentiation of hADSC towards osteoblasts, we investigated the effects of pharmacologic inhibition of GSK-3 on the osteogenic mineralisation capacity of hADSC (Fig. 3). Mineralisation was assessed using Alizarin Red staining and, to allow for accurate inter-assay comparison, an automated image analysis protocol was developed to quantify compound-induced mineralisation relative to DMSO vehicle control (Fig. 3A). While the image analysis protocol was developed through the culture of hADSC in an osteogenic differentiation media; it is important to note that cells exposed to the GSK-3 inhibitors in this study were maintained in a basal media without the addition of osteogenic supplements. Incubation of hADSC with AZD2858, AR79, and AZ13282107 led to a marked increase in osteogenic mineralisation relative to DMSO vehicle control (Figs. 3B and C, Table 1). These data indicate that inhibition of GSK-3 enhances osteogenic differentiation of hADSC.

Bone biomarker changes and bone formation in vivo

Time course study with AZD2858

Biomarkers of bone turnover were altered over 28 days of daily dosing with AZD2858 (30 μmol/kg/day) in rats with statistically significant increases in P1NP and decreases in TRAcP-5b seen from 3 days of treatment and onwards (Fig. 4). P1NP was also elevated at 7 and 28 days but reverted to baseline at 14 and 21 days with AZD2858 (Fig. 4A). Serum TRAcP-5b was significantly decreased in AZD2858 vs vehicle treated animals at all exposure times up to 28 days (Fig. 4B). Additional biomarker measurements showed increases in osteocalcin and Rat Laps (rat equivalent of human CTX) after 14 day treatment with AZD2858 (Supplementary Table 1). Histopathology assessment of H&E stained femur sections observed increases in bone mass (hyperostosis) for all AZD2858 treated groups beyond day 3 with moderate to severe increases in bone mass in animals treated for 14 days or longer. These changes were confirmed by image analysis of H&E stained sections which demonstrated statistically significant increases in bone mass in the epiphysis and metaphysis regions in animals treated for 14 days

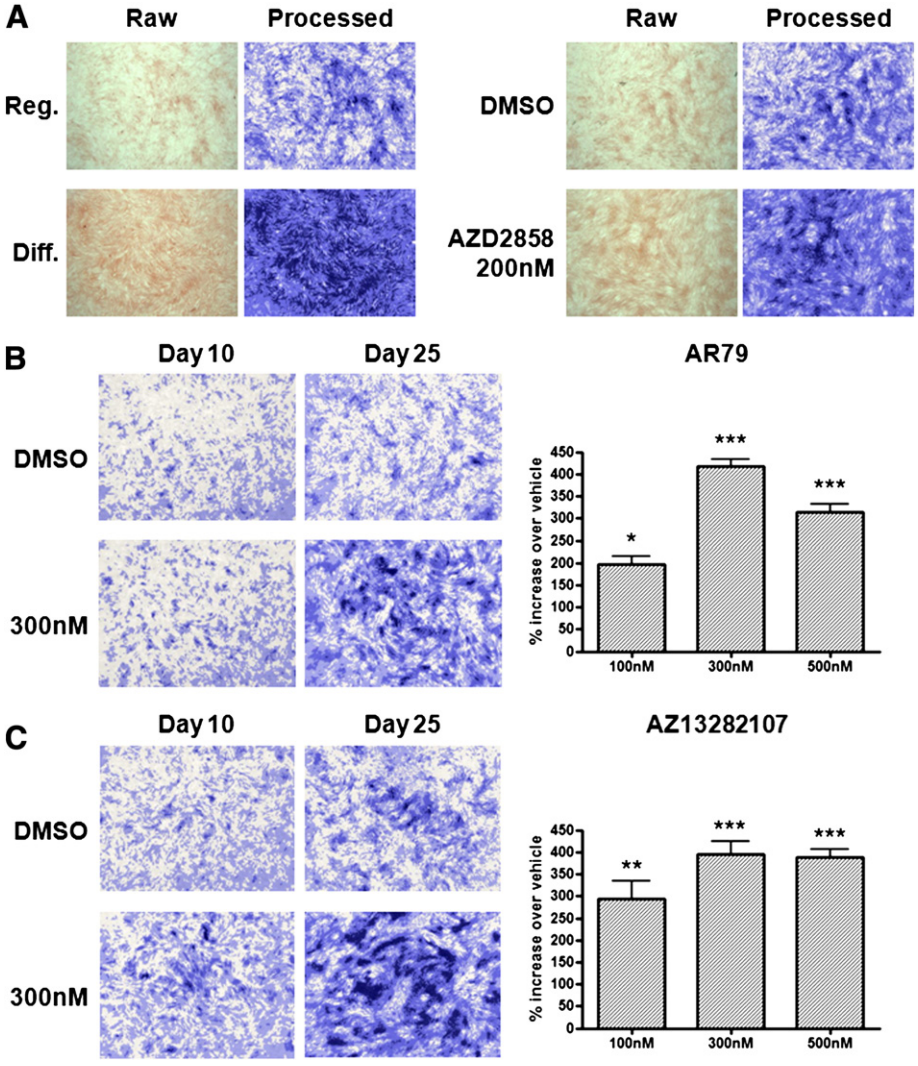

Fig. 3. Osteogenic mineralisation in human ADSC assessed through Alizarin Red staining and quantified using Definiens Developer XD image analysis software. (A) Representative images of osteogenic mineralisation following 26-days in basal (Reg.) or osteogenic (Diff.) media; or 0.2% DMSO vehicle or 200 nM AZD2858. (B) and (C) Representative images of osteogenic mineralisation following 10 and 25 days in basal media and 0.2% DMSO vehicle and (B) 300 nM AR79, or (C) 300 nM AZ13282107 (left); and quantification of mineralisation induced by (B) AR79, or (C) AZ13282107, at day 25 (right). Results expressed as mean ± SEM and analysed by ANOVA followed by Tukey's multiple comparison post-hoc test (n = 3). *p < 0.05; **p < 0.01; ***p < 0.001 *versus* vehicle control.

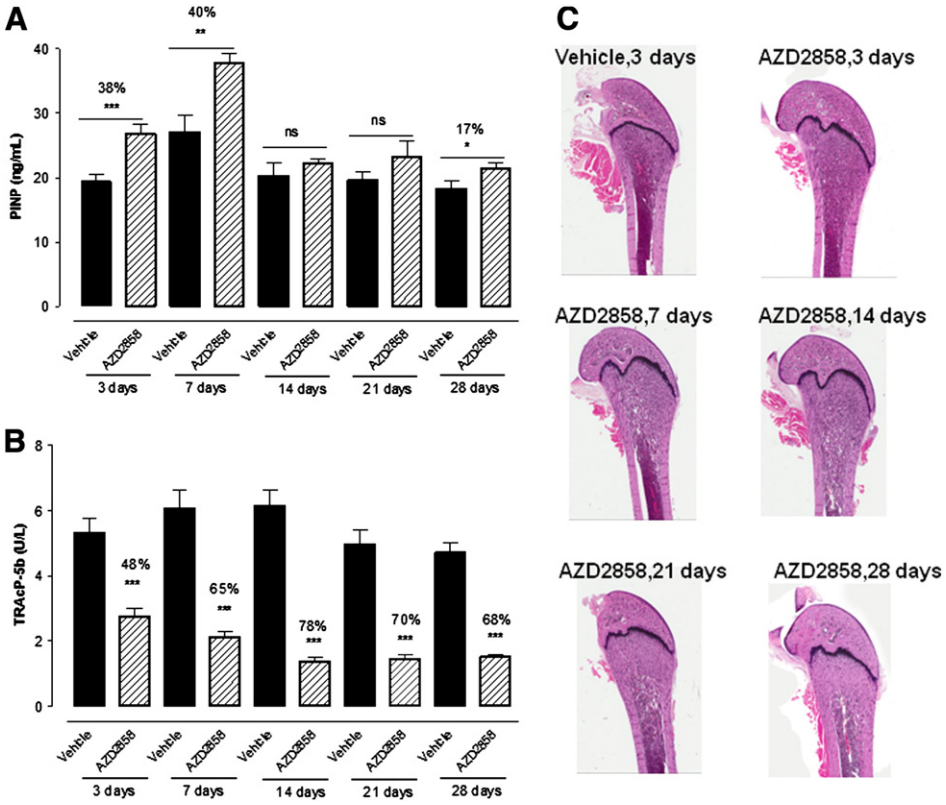

Fig. 4. Time course of serum bone turnover biomarkers and femur histopathology changes with AZD2858 dosed orally for 3, 7, 14, 21 or 28 days. (A) Serum P1NP and (B) TRAcP-5b levels. Results expressed as mean ± SEM, *$p < 0.05$; *$p < 0.01$; ***$p < 0.001$ *versus* relevant vehicle, time match control using Wilcoxon's 2 sided test, $n = 6–8$ per group. (C) Representative images of femurs illustrating progression of hyperostosis during the 28 day treatment period. No effects observed following 3 days treatment with AZD2858, mild hyperostosis following 7 days treatment, moderate effects following 14 day treatment and severe hyperostosis observed following 21 or 28 days treatment. All images are presented as H + E ×1 Aperio Sub-gross Image.

or longer (Supplementary Fig. S2). Hyperostosis was most prominent in the epiphysis and metaphysis and was characterised by an increase in the amount of trabecular bone with a reciprocal decrease in the area of marrow space (Fig. 4C). In some animals, trabeculae extended into the marrow cavity of the diaphysis. These changes were accompanied by a diffuse osteoblast hyperplasia that was characterised by the presence of large activated cells adhering to the endosteal surfaces of bone. Changes in cortical bone were less pronounced with generally only minimal or mild thickening. Therefore, the potential bone anabolic effect of AZD2858, as indicated by the time dependent changes in serum biomarkers, was confirmed by increased bone mass in rat femurs over the 4 week dosing period.

The time course study with AZD2858 demonstrated significant changes in serum bone turnover markers (P1NP and TRAcP-5b) and femur bone formation after only 7 days of daily dosing. Therefore, in subsequent *in vivo* studies, 7 days of dosing with the GSK-3 inhibitors was chosen to assess the activity of AR79 and AZ13282107 on bone turnover and compared with effects of $PTH_{1–34}$ or alendronate. Biomarker changes after 7 days of AR79, AZ13282107, $PTH_{1–34}$ or alendronate are illustrated in Fig. 5. Increases in P1NP and inhibition of TRAcP-5b were seen with AR79 and AZ13282107 compared to vehicle. These biomarker changes were dose related which is consistent with the dose dependent increase in systemic exposure for each compound (Fig. 6). Intermittent dosing with $PTH_{1–34}$ produced an increase in P1NP but did not affect TRAcP-5b (Figs. 5E and F). Conversely, alendronate inhibited TRAcP-5b but did not affect P1NP. In contrast to the effects of $PTH_{1–34}$ and alendronate on bone turnover biomarkers, inhibitors of GSK-3 altered both P1NP and TRAcP-5b serum levels after 7 days.

Femur histopathology assessment after 7 days of GSK-3 inhibitor treatment resulted in a dose-related minimal to moderate increase in bone formation (hyperostosis) with both AR79 or AZ13282107. These changes appeared almost identical to those induced by AZD2858, with the additional finding that in a proportion of animals mild focal increases in the thickness of cortical bone were noted together with synovial membrane hyperplasia and fibroplasia.

14 day biomarker, bone mass & 3D-architecture by μCT

A dose related increase in serum P1NP and inhibition of TRAcP-5b was measured following 14 day treatment with AR79 compared to the vehicle control (Supplementary Figs. S3A and B). Bone formation induced by AR79 following 14 days exposure was determined by femur μCT and pQCT analysis of bone. By pQCT, AR79-mediated bone formation was illustrated by a statistically significant increase in total bone mineral density of 6.6% compared with control animals (Vehicle 764 ± 16: AR79 814 ± 15 mg/cm^3, Supplementary Table 2, Figs. S3C and D). The μCT analysis and quantification of bone mass and structure indicated that AR79 increased trabecular thickness and decreased 3-D connectivity which is consistent with increased bone formation (Supplementary Table 2). Similar studies in mice, demonstrated an increase in femur bone mineral density and bone mineral content as determined by pQCT following 28 day treatment with AR79. Thus, indicating a bone anabolic effect of AR79 in a second rodent species (data not shown).

Discussion

Through *in vitro* and *in vivo* studies using three novel inhibitors of GSK-3, we have demonstrated that GSK-3 inhibition results in commitment of human MSCs towards osteoblasts and mineralisation, a pro-bone formation phenotype that translates *in vivo* to serum bone turnover biomarker changes consistent with increased bone formation and reduced resorption in rats.

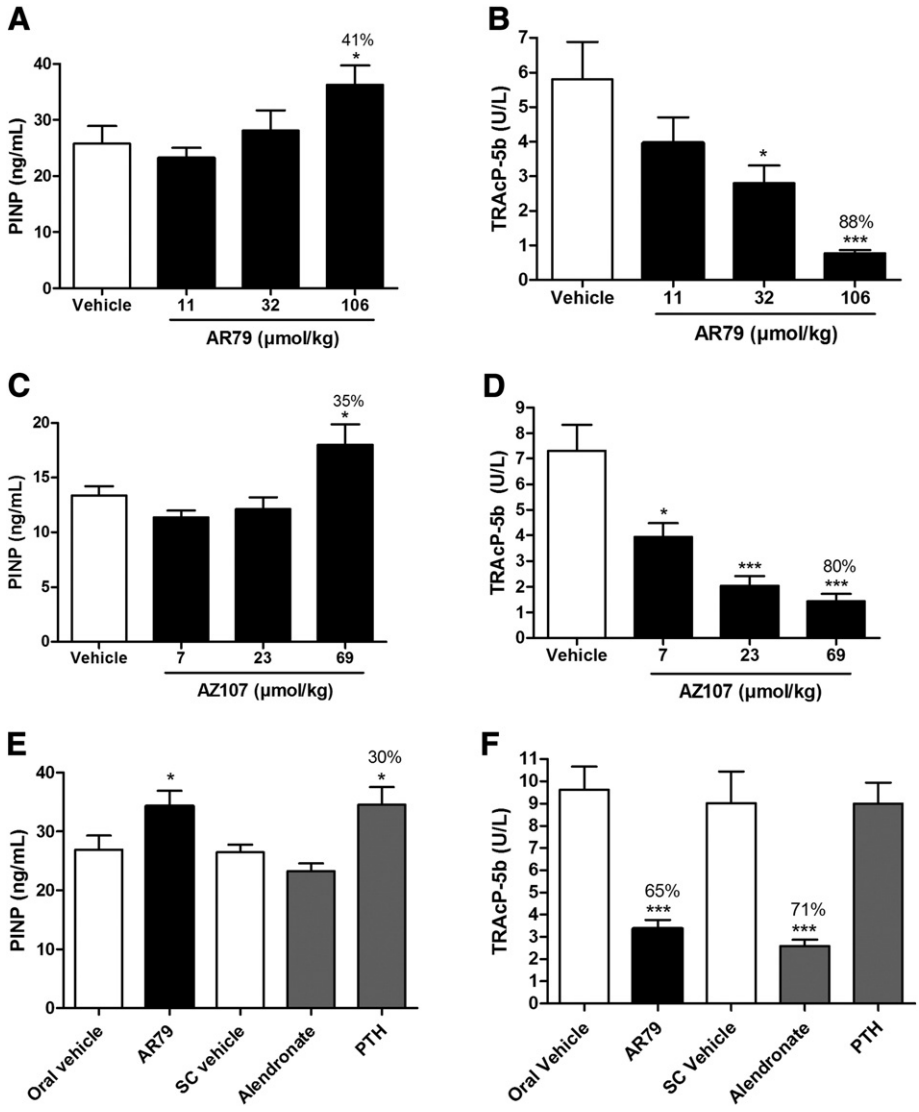

Fig. 5. Differential effects of GSK3 inhibitors, PTH_{1-34} and Alendronate on serum bone turnover biomarkers (P1NP, TRAcP-5b) following 7 days of dosing with AR79, AZ13282107 (AZ107), PTH_{1-34} or Alendronate. (A, B) Rats were dosed with AR79 oral UID, (C,D) AZ107 oral UID or (E, F) AR79 (oral UID), PTH_{1-34} or Alendronate (sc) Results expressed as mean ± SEM, $^{*}p < 0.05$; $^{*}p < 0.01$; $^{***}p < 0.001$ *versus* relevant vehicle control using Mann–Whitney, n = 10 per group.

Modulation of canonical Wnt/β-catenin signalling and its consequences on osteoblastogenesis remain controversial and, while a significant body of literature describe that Wnt/β-catenin activation promotes osteogenic differentiation (Bain et al., 2003; Eijken et al., 2008; Gambardella et al., 2011; Krause et al., 2010; Marsell et al., 2012), it is important to note that there are also reports suggesting

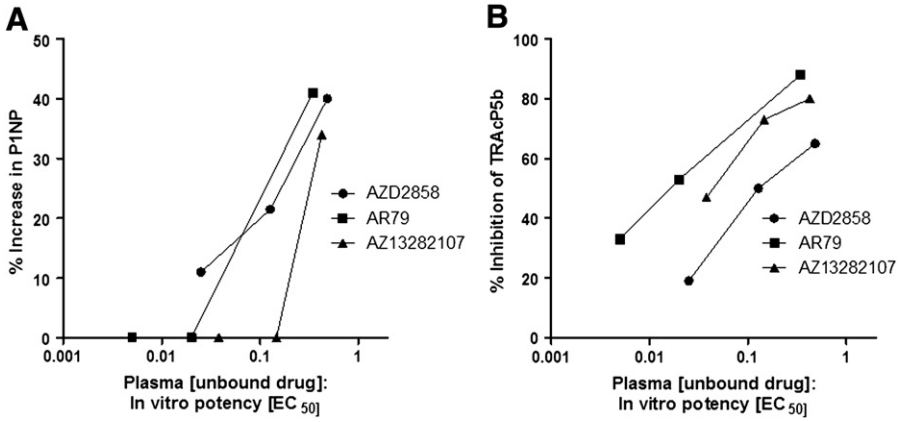

Fig. 6. Relationship between systemic plasma exposure of AZD2858, AR79 and AZ13282107 and serum biomarker changes (A) Serum P1NP and (B) TRAcP-5b levels (samples taken 24 h after 7th oral dose and plasma exposures normalised for differences in potency at GSK-3 and plasma protein binding). Results expressed as mean data for each treatment group.

that the modulation of Wnt/β-catenin signalling with small interfering RNA (siRNA)-mediated GSK-3 silencing and pharmacologic agents inhibits the osteogenic differentiation of mesenchymal stem cells (Huh et al., 2013; Zaragosi et al., 2008). Nevertheless, our studies demonstrate that activation of the Wnt/β-catenin signalling cascade stimulates osteogenesis. Increased TAZ expression is consistent with the commitment of MSCs towards osteoblasts. TAZ has been reported to enhance osteoblastogenesis and suppress the differentiation of MSCs towards adipocytes. In addition, TAZ-deficient MSCs have been shown to be predisposed to adipocyte, rather than osteoblast, differentiation (Hong and Yaffe, 2006; Hong et al., 2005). Where TAZ expression is suppressed, as with elevated tumour necrosis factor-α, the osteogenic potential of MSCs is impaired (Li et al., 2007). Furthermore, recent studies in Wnt-3A-treated murine ST-2 bone marrow stromal cells and primary MSCs exposed to recombinant Dkk-1, an extracellular Wnt antagonist, indicate stimulation of Wnt/β-catenin signalling promotes MSC differentiation towards osteoblasts through stabilisation of TAZ (Azzolin et al., 2012). The canonical Wnt/β-catenin pathway is complex however with its activity regulated by multiple Wnt ligands, Wnt receptors, and numerous soluble inhibitors acting at different points in the signalling cascade to regulate its activity (Clevers and Nusse, 2012). This complexity, combined with the differences in MSC source, species investigated, study protocols, and treatment duration may contribute to the conflicting published data. In our own studies, the increase in osterix expression in hADSC following exposure to GSK-3 inhibitors indicates an increased commitment of cells towards an osteoblast phenotype. However, since recent reports have shown that osterix can itself inhibit the Wnt/β-catenin pathway, possibly through a synergistic interaction with hypoxia-inducible factor-1α (HIF-1α) (Chen et al., 2012; Zhang et al., 2008), further studies are required to understand the temporal effects of GSK-3 inhibition on osteogenesis. Nevertheless, the increased expression of TAZ and osterix and mineralisation in hADSC following treatment with AZD2858, AR79, and AZ13282107 observed in our studies are consistent with the hypothesis that inhibition of GSK-3 promotes osteoblastogenesis.

In healthy rats, repeat dosing with these three novel GSK-3 inhibitors led to changes in two biomarkers of bone metabolism, suggesting an uncoupling of the normal balance between bone resorption and formation, which resulted in a net increase in bone formation. Time dependent changes in several bone biomarkers were observed from day 3 onwards with AZD2858. All three GSK-3 inhibitors produced an increase in P1NP and a reduction in TRAcP-5b after 7 days of dosing in rats which was associated with an increase in bone mass in femurs. The increase in bone mass (imaging/histology) seen with AZD2858 is consistent with previous publications where daily dosing for 2 weeks in normal rats produced an increase in both trabecular and cortical bone mass (Marsell et al., 2012). In mice, AZD2858 has been shown to cause expansion of the mesenchymal progenitor cell compartment with increases in CFU-O and CFU-A in the bone marrow compartment after 3 days of dosing, increases osteoblasts on the endocortical surface of the tibia and bone mass (μCT) at 14 days (Gambardella et al., 2011). Therefore, GSK-3 inhibition with AZD2858 is thought to drive bone anabolism by increasing the progenitor pool and enhancing osteoblast differentiation *in vivo*.

During the formation of bone, P1NP is cleaved from the carboxy terminal of the procollagen molecule on conversion to collagen and is used as a specific and sensitive bone turnover marker for monitoring anabolic treatment in humans (Chen et al., 2005). In our studies, the increase in circulating P1NP seen after 3 and 7 days of dosing with AZD2858 is an early indication of bone formation. This elevated level of circulating P1NP with AZD2858 was not maintained over the 28 day period of dosing and the reason for this is not clear. It is possible that there may be an increased rate of clearance of P1NP from the circulation or perhaps a lower level of bone formation occurs post-7 days which is not detected by changes in circulating P1NP levels. Previous reports discussing similar inconsistent rises in P1NP with longer term dosing of anabolic agents have suggested that early increases in P1NP are followed by modest steady state levels of P1NP (Hale et al., 2007). The other GSK-3 inhibitors (AR79 and AZ13282107) and intermittent dosing with PTH_{1-34} produced an increase in circulating P1NP at day 7, suggestive of a bone anabolic phenotype with these molecules.

The primary biomarkers of bone resorption are degradation products of type 1 collagen such as C-telopeptide of type 1 collagen. AZD2858 only produced a significant increase in RatLAPS (rat CTX) at 14 days of treatment which is similar to a previous report (Marsell et al., 2012). In contrast, serum TRAcP-5b was reduced by day 3 and maintained throughout the duration of the time course with AZD2858 treatment. Therefore, this latter biomarker was used to investigate the effect of the other two GSK-3 inhibitors as well as PTH_{1-34} and alendronate. Two forms of TRAcP enzyme, TRAcP-5a and TRAcP-5b are expressed in macrophages and osteoclasts respectively (Janckila et al., 2002). Although the involvement of TRAcP in the process of bone resorption has not been fully elucidated, TRAcP is released in significant quantities by bone resorbing osteoclasts and TRAcP release is clearly correlated with the extent of bone resorption (Kirstein et al., 2006). TRAcP levels are correlated to osteoclast numbers and TRAcP levels are elevated in the serum of individuals who have a high rate of bone resorption (Halleen et al., 2002). A dose related inhibition of TRAcP-5b was seen with AZD2858, AR79 and AZ13282107 and Alendronate at 7 days suggesting an anti-resorptive component to the activity of the GSK-3 inhibitors as well as the bisphosphonate. There are several different ways that GSK-3 inhibition may affect bone resorption either directly (*e.g.* by altering osteoclast numbers/function) or indirectly. Mice expressing a stabilised form of β-catenin in osteoblasts, exhibit osteopetrosis and reduced numbers of osteoclasts staining positive for TRAcP (Glass et al., 2005). This may be due to upregulation of osteoprotegerin in osteoblastic cells which in turn inhibits osteoclast differentiation and bone resorption (Glass et al., 2005). However, there is contrasting data where catalytically inactive GSK-3β (GSK3β-K85R) or small interfering RNA (siRNA)-mediated GSK-3β silencing enhances osteoclast formation induced by RANKL *in vitro* (Jang et al., 2011). GSK-3 inhibition led to increased bone mass in both mice and rats dosed daily with AZD2858 (Gambardella et al., 2011; Marsell et al., 2012). In mice, increased osteoclast number in the tibial corticoendosteal surface was seen at day 14 with AZD2858 even though an overall increase in bone mass was observed (Gambardella et al., 2011). However, no change in osteoclast numbers was observed with AZD2858 treatment in rats whereas both bone mass and strength increased (Marsell et al., 2012). In the *in vivo* studies described in this manuscript, the overall effect on bone turnover was bone anabolic confirming the bone findings with other GSK-3 inhibitors. Additional investigative work is required to further elucidate the role of GSK-3 in osteoclast function and bone resorption in normal bone turnover as well as in the disease setting *in vivo*.

GSK-3 inhibition with AZD2858, AR79 and AZ13282107 induced early changes in systemic P1NP and TRAcP-5b serum biomarkers of bone turnover which were associated with histological changes in femurs suggestive of bone formation at day 7. This early biomarker profile observed with GSK-3 inhibition in rats was distinct from classic anti-resorptive bisphosphonate or anabolic PTH_{1-34} treatment. Longer term dosing with AR79 over 14 days led to increased bone mass in femurs which is similar to studies in normal mice and rats treated with AZD2858 (Gambardella et al., 2011; Marsell et al., 2012) and consistent with modulation of the wnt pathway using PTH, lithium chloride and suppression of DKK1 (Clement-Lacroix et al., 2005; Monroe et al., 2012). The bone changes seen with these GSK-3 inhibitors are most likely to be due to inhibition of GSK-3 rather than an off-target effect as all three compounds are potent GSK-3 inhibitors which increase wnt signalling and stimulate mineralisation *in vitro*. Also, these findings are consistent with other GSK-3 inhibitors. In addition, both AZD2858 and AZ13282107 are >70× fold selective for GSK-3 over other kinases

including HIPK2. AR79 does have equipotent activity with HIPK2 but this enzyme currently is not known to have a role in bone remodelling.

Conclusion

These results indicate that GSK-3 inhibition causes MSC commitment and differentiation to osteoblasts in human cells and produced a net increase in bone formation consistent with the role of the canonical Wnt signalling pathway in skeletal formation in rats. Serum biomarkers of bone turnover, P1NP and TRAcP-5b, are early indicators of bone turnover modulation in rats treated with GSK-3 inhibitors which may also be useful clinical indicators of efficacy within human studies.

Supplementary data to this article can be found online at http://dx.doi.org/10.1016/j.taap.2013.07.001.

Conflict of interest

No competing interests.

Acknowledgments

Thanks to Ashwani Bahl, Witte Koopmann and Paul Newbold for their scientific advice and to Martyn Foster for his contributions to the pathology discussions. Also, we'd like to acknowledge the important technical contribution of Alison Bigley, Adrian Freeman and Jo Francis to this work.

Authors' role: All authors were involved in the preparation, review and approval of this manuscript: MF, JEP, PJO to the design, implementation, analysis and interpretation of the *in vitro* assays: PSG, KJE and SK design, implementation and interpretation of rat efficacy studies and similarly to PFC for the pharmacokinetic evaluations. PAH for the histopathology assesment of *in vivo* studies. HS and HW for their chemistry input to the design and synthesis of the compounds as well as scientific contribution to this experimental work.

References

Azzolin, L., Zanconato, F., Bresolin, S., Forcato, M., Basso, G., Bicciato, S., Cordenonsi, M., Piccolo, S., 2012. Role of TAZ as mediator of Wnt signaling. Cell 151, 1443–1456.

Bain, G., Müller, T., Wang, X., Papkoff, J., 2003. Activated β-catenin induces osteoblast differentiation of C3H10T1/2 cells and participates in BMP2 mediated signal transduction. Biochem. Biophys. Res. Commun. 301, 84–91.

Chen, P., Satterwhite, J.H., Licata, A.A., Lewiecki, E.M., Sipos, A.A., Misurski, D.M., Wagman, R.B., 2005. Early changes in biochemical markers of bone formation predict BMD response to teriparatide in postmenopausal women with osteoporosis. J. Bone Miner. Res. 20, 962–970.

Chen, D., Li, Y., Zhou, Z., Xing, Y., Zhong, Y., Zou, X., Tian, W., Zhang, C., 2012. Synergistic inhibition of Wnt pathway by HIF-1α and osteoblast-specific transcription factor Osterix (Osx) in osteoblasts. PLoS One 7, e52948.

Clement-Lacroix, P., Ai, M., Morvan, F., Roman-Roman, S., Vayssiere, B., Belleville, C., Estrera, K., Warman, M.L., Baron, R., Rawadi, G., 2005. Lrp5-independent activation of Wnt signaling by lithium chloride increases bone formation and bone mass in mice. Proc. Natl. Acad. Sci. U. S. A. 102, 17406–17411.

Clevers, H., Nusse, R., 2012. Wnt/β-catenin signaling and disease. Cell 149, 1192–1205.

Eijken, M., Meijer, I.M., Westbroek, I., Koedam, M., Chiba, H., Uitterlinden, A.G., Pols, H.A., van Leeuwen, J.P., 2008. Wnt signalling acts and is regulated in a human osteoblast differentiation dependent manner. J. Cell. Biochem. 104, 568–579.

Fukata, S., Hagino, H., Okano, T., Yamane, I., Kameyama, Y., Teshima, R., 2004. Effect of intermittent administration of human parathyroid hormone on bone mineral density and arthritis in rats with collagen-induced arthritis. Arthritis Rheum. 50, 4060–4069.

Gambardella, A., Nagaraju, C.K., O'Shea, P.J., Mohanty, S.T., Kottam, L., Pilling, J., Sullivan, S., Djerbi, M., Koopmann, W., Croucher, P.I., Bellantuono, I., 2011. Glycogen synthase kinase-3α/β inhibition promotes *in vivo* amplification of endogenous mesenchymal progenitors with osteogenic and adipogenic potential and their differentiation to the osteogenic lineage. J. Bone Miner. Res. 26, 811–821.

Glass II, D.A., Bialek, P., Ahn, J.D., Starbuck, M., Patel, M.S., Clevers, H., Taketo, M.M., Long, F., McMahon, A.P., Lang, R.A., Karsenty, G., 2005. Canonical Wnt signaling in differentiated osteoblasts controls osteoclast differentiation. Dev. Cell 8, 751–764.

Hale, L.V., Sells Galvin, R.J., Risteli, J., Harvey, A.K., Yang, X., Cain, R.L., Zeng, Q., Frolik, C.A., Sato, M., Schidt, A.L., Geiser, A.G., 2007. PINP: a serum biomarker of bone formation in the rat. Bone 40, 1103–1109.

Halleen, J.M., Ylipahkala, H., Alatalo, S.L., Janckila, A.J., Heikkinen, J.E., Suominen, H., Cheng, S., Vaananen, H.K., 2002. Serum tartrate-resistant acid phosphatase 5b, but not 5a, correlates with other markers of bone turnover and bone mineral density. Calcif. Tissue Int. 71, 20–25.

Halleen, J.M., Tiitinen, S.L., Ylipahkala, H., Fagerlund, K.M., Vaananen, H.K., 2006. Tartrate-resistant acid phosphatase 5b (TRACP 5b) as a marker of bone resorption. Clin. Lab. 52, 499–509.

Harada, H., Nakayama, T., Nanaka, T., Katsumata, T., 2004. Effects of bisphosphonates on joint damage and bone loss in rat adjuvant-induced arthritis. Inflamm. Res. 53, 45–52.

Hartmann, C.A., 2006. Wnt canon orchestrating osteoblastogenesis. Trends Cell Biol. 16, 151–158.

Hong, J.H., Yaffe, M.B., 2006. TAZ: a beta-catenin-like molecule that regulates mesenchymal stem cell differentiation. Cell Cycle 5, 176–179.

Hong, J.H., Hwang, E.S., McManus, M.T., Amsterdam, A., Tian, Y., Kalmukova, R., Mueller, E., Benjamin, T., Spiegelman, B.M., Sharp, P.A., Hopkins, N., Yaffe, M.B., 2005. TAZ, a transcriptional modulator of mesenchymal stem cell differentiation. Science 309, 1074–1078.

Huh, J.-E., Ko, R., Jung, H.J., Lee, S.Y., 2013. Glycogen synthase kinase 3β promotes osteogenic differentiation of murine adipose-derived stromal cells. PLoS One 8, e54551.

Janckila, A.J., Neustadt, D.H., Nakasato, Y.R., Halleen, J.M., Hentunen, T., Yam, L.T., 2002. Serum tartrate-resistant acid phosphatase isoforms in rheumatoid arthritis. Clin. Chim. Acta 320, 49–58.

Jang, H.D., Shin, J.H., Park, D.R., Hong, J.H., Yoon, K., Ko, R., Ko, C.Y., Kim, H.S., Jeong, D., Kim, N., Lee, S.Y., 2011. Inactivation of glycogen synthase kinase-3β is required for osteoclast differentiation. Biol. Chem. 286, 39043–39050.

Kirstein, B., Chambers, T.J., Fuller, K., 2006. Secretion of tartrate-resistant acid phosphatase by osteoclasts correlates with resorptive behavior. J. Cell. Biochem. 98, 1085–1094.

Krause, U., Harris, S., Green, A., Ylostalo, J., Zeitouni, S., Lee, N., Gregory, C.A., 2010. Pharmaceutical modulation of canonical Wnt signalling in multipotent stromal cells for improved osteoinductive therapy. Proc. Natl. Acad. Sci. U. S. A. 107, 4147–4152.

Kugimiya, F., Kawaguchi, H., Ohba, S., Kawamura, N., Hirata, M., Chikuda, H., Azuma, Y., Woodgett, J.R., Nakamura, K., Chung, U.I., 2007. GSK-3beta controls osteogenesis through regulating Runx2 activity. PLoS One 2, e837.

Kulkarni, N.H., Onyia, J.E., Zeng, Q., Tian, X., Liu, M., Halladay, D.L., Frolik, C.A., Engler, T., Wei, T., Kriauciunas, A., Martin, T.J., Sato, M., Bryant, H.U., Ma, Y.L., 2006. Orally bioavailable GSK-3alpha/beta dual inhibitor increases markers of cellular differentiation *in vitro* and bone mass *in vivo*. J. Bone Miner. Res. 21, 910–920.

Li, B., Shi, M., Li, J., Zhang, H., Chen, B., Chen, L., Gao, W., Giuliani, N., Zhao, R.C., 2007. Elevated tumor necrosis factor-α suppresses TAZ expression and impairs osteogenic potential of Flk-1+ mesenchymal stem cells in patients with multiple myeloma. Stem Cells Dev. 16, 921–930.

Marsell, R., Sisask, G., Nilsson, Y., Sundgren-Andersson, A.K., Andersson, U., Larsson, S., Nilsson, O., Ljunggren, O., Jonsson, K.B., 2012. GSK-3 inhibition by an orally active small molecule increased bone mass in rats. Bone 50, 619–627.

Monroe, D.G., McGee-Lawrence, M.E., Oursler, M.J., Westendorf, J.J., 2012. Update on Wnt signaling in bone cell biology and bone disease. Gene 492, 1–18.

Nakashima, K., Zhou, X., Kunkel, G., Zhang, Z., Deng, J.M., Behringer, R.R., de Crombrugghe, B., 2002. The novel zinc finger-containing transcription factor Osx is required for osteoblast differentiation and bone formation. Cell 108, 17–29.

Reinhold, M.I., Naski, M.C., 2007. Direct interactions of Runx2 and canonical Wnt signaling induce FGF18. J. Biol. Chem. 282, 3653–3663.

Theriault, R.L., 2012. Biology of bone metastases. Cancer Control 19, 92–101.

Tuukkanen, J., Koivukangas, A., Jämsä, T., Sundquist, K., Mackay, C.A., Marks Jr., S.C., 2000. Mineral density and bone strength are dissociated in long bones of rat osteopetrotic mutations. J. Bone Miner. Res. 15, 1905–1911.

Zaragosi, L.E., Wdziekonski, B., Fontaine, C., Villageois, P., Peraldi, P., Dani, C., 2008. Effects of GSK3 inhibitors on *in vitro* expansion and differentiation of human adipose-derived stem cells into adipocytes. BMC Cell Biol. 9, 11.

Zhang, C., Cho, K., Huang, Y., Lyons, J.P., Zhou, X., Sinha, K., McCrea, P.D., de Crombrugghe, B., 2008. Inhibition of Wnt signalling by the osteoblast-specific transcription factor Osterix. Proc. Natl. Acad. Sci. U. S. A. 105, 6936–6941.